

## Article

# Hydrogels Are Reinforced with Colombian Fique Nanofibers to Improve Techno-Functional Properties for Agricultural Purposes

Marcelo A. Guancha-Chalapud <sup>1</sup>, Liliana Serna-Cock <sup>2</sup>  and Diego F. Tirado <sup>3,\*</sup> 

<sup>1</sup> Centro Nacional de Asistencia Técnica a la industria (ASTIN), Servicio Nacional de Aprendizaje (SENA), Cali 760004, Colombia; marceloguanca@misena.edu.co

<sup>2</sup> Faculty of Engineering and Administration, Universidad Nacional de Colombia, Sede Palmira, Palmira 763533, Colombia; lserna@unal.edu.co

<sup>3</sup> Dirección Académica, Universidad Nacional de Colombia, Sede de La Paz, La Paz 202017, Colombia

\* Correspondence: dtiradoa@unal.edu.co

**Abstract:** Colombia is the world's largest producer of fique fibers (*Furcraea bedinghausii*), with a net production of 30,000 tons per year. This work proposes to revalue waste from the Colombian fique agroindustry. For this purpose, cellulose nanofibers were obtained from fique and used as reinforcement material to create acrylic superabsorbent hydrogels. Unreinforced acrylic hydrogels (AHR0) and acrylic hydrogels reinforced with fique nanofibers at 3% *w/w* (AHR3), 5% *w/w* (AHR5), and 10 % *w/w* (AHR10) were synthesized using the solution polymerization method. The best hydrogel formulation for agricultural purposes was chosen by comparing their swelling behavior, mechanical properties, and using scanning electron microscopy (SEM). By raising the nanofiber concentration to 3% (AHR3), the best-chosen formulation, the interaction between the nanofibers and the polymer matrix increased, which favored the network stability. However, beyond AHR3, there was a higher viscosity of the reactive system, which caused a reduction in the mobility of the polymer chains, thus disfavoring the swelling capacity. The reinforced hydrogel proposed in this study (AHR3) could represent a contribution to overcoming the problems of land dryness present in Colombia, an issue that will worsen in the coming years due to the climate emergency.

**Keywords:** global water crisis; sustainability; bioprospecting; circular economy; agro-industrial waste revalorization; bioeconomy; superabsorbent hydrogel; nanofiber



**Citation:** Guancha-Chalapud, M.A.; Serna-Cock, L.; Tirado, D.F. Hydrogels Are Reinforced with Colombian Fique Nanofibers to Improve Techno-Functional Properties for Agricultural Purposes. *Agriculture* **2022**, *12*, 117. <https://doi.org/10.3390/agriculture12010117>

Academic Editor: Dongwei Gui

Received: 24 December 2021

Accepted: 12 January 2022

Published: 14 January 2022

**Publisher's Note:** MDPI stays neutral with regard to jurisdictional claims in published maps and institutional affiliations.



**Copyright:** © 2022 by the authors. Licensee MDPI, Basel, Switzerland. This article is an open access article distributed under the terms and conditions of the Creative Commons Attribution (CC BY) license (<https://creativecommons.org/licenses/by/4.0/>).

## 1. Introduction

Since 2017, the United Nations (UN) has projected the world population to reach 8.6 billion in 2030, 9.8 billion in 2050, and 11.2 billion in 2100, driven by growth in developing countries such as Colombia [1]. According to the intergovernmental organization, by 2020, 13% of the world population could be going hungry due to man-made conflicts, the climate emergency, economic downturns, and, of course, the COVID-19 pandemic [2]. If trends continue, by 2050, the world will have 2 billion additional hungry people [3] and a severe water crisis [4–6], since the planet will require roughly 95% of fresh water for agriculture production [7]. This means that the global food and agricultural systems must seek solutions to optimize water use [8–10]; superabsorbent hydrogels could make a contribution in this regard [11].

Hydrogels are polymers with crisscrossed three-dimensional structures that allows water molecules to be absorbed, stored and released [12,13]. Recently, hydrogels have proven to be versatile for food [14] and agricultural [11,15,16] purposes. In fact, the global hydrogel market was valued at USD 22.1 billion in 2019 and is projected to reach USD 31.4 billion by 2027, growing at a compound annual growth rate (CAGR) of 6.7%

from 2020 to 2027 due to the increased demand for personal, healthcare, hygienic, and agricultural products [17].

Hydrogels used for agricultural applications are synthesized based on acrylates or similar monomers (acrylamide and methyl methacrylate, among others) due to their high swelling capacity and kinetics, their toxic and biological inertness, and their ability to preserve their shape [18]. They also increase the water available in soil, induce the rapid growth of plant stems and leaves, prolong survival under water stress, and allow the controlled release of fertilizers [19]. However, one of the main limitations in the use of hydrogels for agricultural applications is their low mechanical resistance [20]. Since biocompatibility depends on the water content in a swollen hydrogel, swelling studies are important [21]; thus, theoretical and experimental work on hydrogel properties in aqueous media should be performed.

The pressure exerted by the plant and the soil layer on the hydrogel influence the loss of swelling capacity, elasticity, and stiffness. To maintain polymer elasticity, long-chain molecules and adequate interbreeding are needed to dissipate external mechanical stresses on a hydrogel [18]. An alternative is the use of micro/nano-scale cellulose as a reinforcement material in hydrogels [20]. The addition of nanofibers in hydrogels increases compression resistance by up to 50% [22], and the ability to recover its original shape (elasticity) from the application of external forces, up to 80% compared to its original height [22,23].

Through the use of circular economy and revalorization strategies, abundant and biodegradable agro-industrial waste could play an important role in a globally sustainable future economy. Thus, available, sustainable, and inexpensive cellulose sources should be considered for the production of cellulose nanofibers as reinforcing agents [24]. In this regard, Colombia is the world's largest producer of fique (*Furcraea bedinghausii*) fibers, with a net production of 30,000 tons per year. However, the fibers only represent 5% of the weight of fique leaves, while the remaining by-products lack commercial applications and are typically disposed of in surface waters, causing pollution and serious environmental damage [25]. These by-products include tow (8%), pulp (17%), and juice (70%). Fique pulp and tow, raw materials used in this work, are mainly composed of cellulose, hemicellulose, and lignin [26]. The cellulose content in these two fique by-products ranges from 30% to 70% depending on the species, season, and age of the plant [25,26].

In a previous study [24], this research group obtained cellulose nanofibers from the by-products generated by a Colombian fique farm by using chemical methods combined with ultrasound technology. On that occasion, the work mentioned the possibility of revalorizing the by-products to produce cellulose nanofibers that could be used as a reinforcement material in acrylic hydrogels.

This time, our research focused on revaluing fique by-products based on a circular economy model. For this, cellulose nanofibers were obtained from fique by-products (pulp and tow) and used as reinforcement material to create acrylic superabsorbent hydrogels. Unreinforced acrylic hydrogels (AHR0) and acrylic hydrogels reinforced with fique nanofibers at 3% *w/w* (AHR3), 5% *w/w* (AHR5), and 10% *w/w* (AHR10) were synthesized using the solution polymerization method. In the following sections, the best hydrogel formulation for agricultural purposes was chosen by comparing techno-functional properties of AHR0, AHR3, AHR5, and AHR10 analyzed by studying their swelling behavior, mechanical properties, and using scanning electron microscopy (SEM).

## 2. Materials and Methods

### 2.1. Reagents

Sodium hydroxide (NaOH, pellets, Merck, Darmstadt, Germany), sodium chlorite (NaClO<sub>2</sub>, crystals, Sigma-Aldrich, St. Louis, MO, USA), glacial acetic acid (CH<sub>3</sub>COOH, 99.7%, Merck, Darmstadt, Germany), sulfuric acid solution in water type II (H<sub>2</sub>SO<sub>4</sub>, 96%, Merck, Darmstadt, Germany), acrylamide (Crystals, Sigma-Aldrich, St. Louis, MO, USA), acrylic acid (99%, Merck, Darmstadt, Germany), potassium hydroxide (KOH, Pellets, Merck, Darmstadt, Germany), potassium persulfate (K<sub>2</sub>S<sub>2</sub>O<sub>8</sub>, crystals, Panreac, Barcelona, Spain),

N,N'-methylenebis(acrylamide) (NMBA, Crystals, Sigma-Aldrich, St. Louis, MO, USA), and nitrogen (99.99%, Linde, Dublin, Ireland) were all used. All materials were used as received. Unless otherwise specified, the water used in this work was distilled and came from our laboratory.

## 2.2. Raw Material

In this work, fique pulp and tow, by-products of the fique fiber agroindustry of San Bernardo (Nariño, Colombia), were used. The raw material was washed with water. Then, the sample was dried at 65 °C in a forced convection oven (UN 110, Memmert, Schwabach, Germany) until a constant weight was reached. Finally, the dried samples were cut into cubes with an average thickness of 4 mm.

## 2.3. Nanofibers Production

Nanofibers from fique by-products were obtained according to our previous report [24] with slight modifications.

### 2.3.1. Chemical Treatment of the Raw Material

The raw material was both delignified and blanched. For delignification, the sample was mixed (1:25 ratio) with a 4% *w/v* aqueous NaOH solution at 600 rpm and 90 °C for 4 h (Corning, NY, USA). Finally, the mixture was vacuum filtered, and the fibers obtained were washed with water (1:1 ratio) until the pH of the filtrate was in the range of 6 to 7, which was checked with universal pH Indicator strips (Merck, Darmstadt, Germany).

For blanching, the delignified material was mixed (1:20 ratio) with a solution resulting from the mixture (1:1 ratio) of a 1.7% *w/v* aqueous NaClO<sub>2</sub> solution and an acetate buffer solution (27 g NaOH + 75 mL CH<sub>3</sub>COOH L water<sup>-1</sup>). Afterwards, this solution was stirred at 600 rpm and 80 °C for 6 h. Both alkali and bleaching treatments were performed in duplicate. Finally, the fibers were vacuum filtered (Millipore, Merck, Germany), washed with water (1:1 ratio) until neutral pH was reached, and dried in an oven at 50 °C until constant weight was achieved.

### 2.3.2. Obtaining Nanofibers

To obtain nanofibers, 5 g of previously obtained samples was stirred at 400 rpm with 125 mL of H<sub>2</sub>SO<sub>4</sub> 6,5 M for 24 h at 50 °C. Then, the mixture was diluted in 300 mL of water and neutralized with 1600 mL of 4% aqueous NaOH solution. Afterwards, the precipitate was vacuum filtered (Millipore, Merck, Darmstadt, Germany), washed with water (1:1 ratio) and dried at 50 °C for 24 h. Using this dried sample, 100 mL of an aqueous suspension (1% *w/v*) was prepared and mixed well with an ULTRA-TURRAX (T25, IKA, Königswinter, Germany) at 10,000 rpm for 15 min. Afterwards, suspensions were ultrasonically homogenized (Branson SFX550, Emerson, St. Louis, MO, USA) with a  $\frac{1}{2}$ " diameter cylindrical probe at 20 kHz and 550 W for 30 min. The sample temperature was kept between 25 °C and 30 °C in an ice bath. The obtained nanofiber suspensions were freeze dried (Freezone 6 Plus, Labconco, Kansas City, MO, USA) at an ice condenser temperature of −40 °C and a pressure of 0.01 mbar for 24 h. Finally, the nanofibers were stored in hermetic containers at 5 °C for further analysis.

## 2.4. Reinforcing Hydrogels

Non-reinforced acrylic hydrogels (AHR0) and acrylic hydrogels reinforced with 3 % *w/w* (AHR3), 5 % *w/w* (AHR5), and 10 % *w/w* (AHR10) fique nanofiber suspensions previously obtained were synthesized using the solution polymerization method proposed by Zhong et al. [27] with slight modifications. The fique nanofiber percentage is displayed with respect to monomers.

The reaction was performed in a 500 mL ground-glass lid reactor equipped with reflux, nitrogen inlet and outlet, and magnetic stirring. Batches of 200 mL were prepared. Monomer solution was made by mixing 14 g of acrylamide with 22 g of potassium acrylate,

which was previously obtained by neutralizing 16 g of acrylic acid with a KOH solution. Batches of 200 mL were prepared. First, 80 mL nanofiber suspensions (AHR0, AHR3, AHR5, and AHR10) were dispersed using ULTRA-TURRAX at 9000 rpm for 10 min. Then, nanofiber suspension and monomer solutions were mixed and stirred for 10 min. Afterwards,  $K_2S_2O_8$  (0.3% by weight with respect to the monomers) as an initiator and NMBA (0.085% by weight with respect to the monomers) as a crosslinker were added to the mixture. Subsequently, 200 mL of suspension was put in a volumetric flask, brought to reflux, and bubbled with 20 mL of nitrogen  $\text{min}^{-1}$  for 20 min. Finally, the system was heated at 70 °C for 6 h to complete the polymerization reaction. The final product was cut into 1 mm to 2 mm width cubes and washed with ethanol (1:2 ratio) and dried at 70 °C until constant weight was achieved.

### 2.5. Choosing the Best Hydrogel Formulation

The best hydrogel formulation for agricultural purposes was chosen subjectively by comparing the techno-functional properties of AHR0, AHR3, AHR5, and AHR10 analyzed by studying their swelling behavior, mechanical properties, and scanning electron microscopy (SEM).

#### 2.5.1. Swelling Study

The swelling behavior of AHR0, AHR3, AHR5, and AHR10 was analyzed according to the methodology proposed by Karadag et al. [21] and Spagnol et al. [12,13] with modifications. For this, 0.2 g of dried hydrogel was soaked on a 400-mesh sieve in distilled water for 5 min, 10 min, 15 min, 30 min, 60 min, 90 min, 120 min, 180 min, 240 min, 300 min, and 360 min. The surface water was removed with a cloth. The swollen material was weighed; subsequently, the swelling ratio was calculated according to Equation (1).

$$W = \frac{m_t - m_0}{m_0} \quad (1)$$

where  $W$  is the swelling ratio at time  $t$  (g  $\text{H}_2\text{O}$ /g hydrogel),  $m_t$  is the mass of the swollen material at time  $t$  (g), and  $m_0$  is the mass of the dried material (g).

For the swelling of polymers, such as those used in this work, the second-order kinetic relationship shown in Equation (2) can be used.

$$\frac{t}{W} = A + Bt \quad (2)$$

where the reciprocal of the initial swelling rate ( $A$ ) and the inverse of the maximum or equilibrium swelling ( $B$ ) are described by Equations (3) and (4), respectively.

$$A = \left( \frac{\partial W}{\partial t} \right)_0 = \frac{1}{k_S W_t^2} \quad (3)$$

$$B = \frac{1}{W_t} \quad (4)$$

where  $k_S$  is the swelling rate constant [(g  $\text{H}_2\text{O}$  g hydrogel $^{-1}$ )  $\text{min}^{-1}$ ], and  $W_t$  is a theoretical swelling value at equilibrium (g  $\text{H}_2\text{O}$  g hydrogel $^{-1}$ ). Finally, the initial swelling rate can be described by Equation (5).

$$k_{is} = k_S W_{eq}^2 \quad (5)$$

where  $k_{is}$  is the equilibrium swelling [(g  $\text{H}_2\text{O}$  g hydrogel $^{-1}$ )  $\text{min}^{-1}$ ], and  $W_{eq}$  is the swelling value at equilibrium (g  $\text{H}_2\text{O}$  g hydrogel $^{-1}$ ).

#### 2.5.2. Mechanical Properties

The maximum compression resistance ( $R_C$ ) and strain percent of hydrogel formulations were measured in a universal testing machine (Good brand 50 IR, Germany) with

a 100 N load cell and a 10 cm diameter circular compression, at a deformation speed of  $1 \text{ mm min}^{-1}$ . Samples were cut into cylindrical shapes ( $25 \times 25 \text{ mm}$ ) at their maximum swelling ratio.

### 2.5.3. Scanning Electron Microscopy (SEM)

Hydrogel formulations were observed with a scanning electron microscope (SEM, JEOL Model JSM-6490, Peabody, MA, USA) with an acceleration voltage of 20 kV and high vacuum conditions. Additionally, samples were embedded in resin, their water content was extracted by lyophilization, and they were coated with gold to study their morphology.

### 2.6. Experimental Design and Statistical Analysis

A single-factor, completely randomized design was implemented. This factor was set as the concentration of fique nanofibers used to reinforce the hydrogel. For this, a non-reinforced acrylic hydrogel (AHR0) and acrylic hydrogels reinforced with 3% *w/w* (AHR3), 5% *w/w* (AHR5), and 10% *w/w* (AHR10) fique nanofiber were tested. Experiments were performed in triplicate, and the analyses were repeated twice ( $n = 2 \times 3$ ). The mean and standard deviation were calculated for all data. Response variables were submitted to analysis of variance (ANOVA). When statistical differences at a significance level of 5% ( $p \leq 0.05$ ) were found, Tukey's analysis was performed to determine the influence of the selected factors. Data processing was carried out using Minitab 18 statistical program (Minitab, State College, PA, USA).

## 3. Results and Discussions

### 3.1. Swelling Behavior

Swelling isotherms of acrylic hydrogels and acrylic hydrogels reinforced with fique nanofibers, synthesized using the solution polymerization method, are plotted and shown in Figure 1.

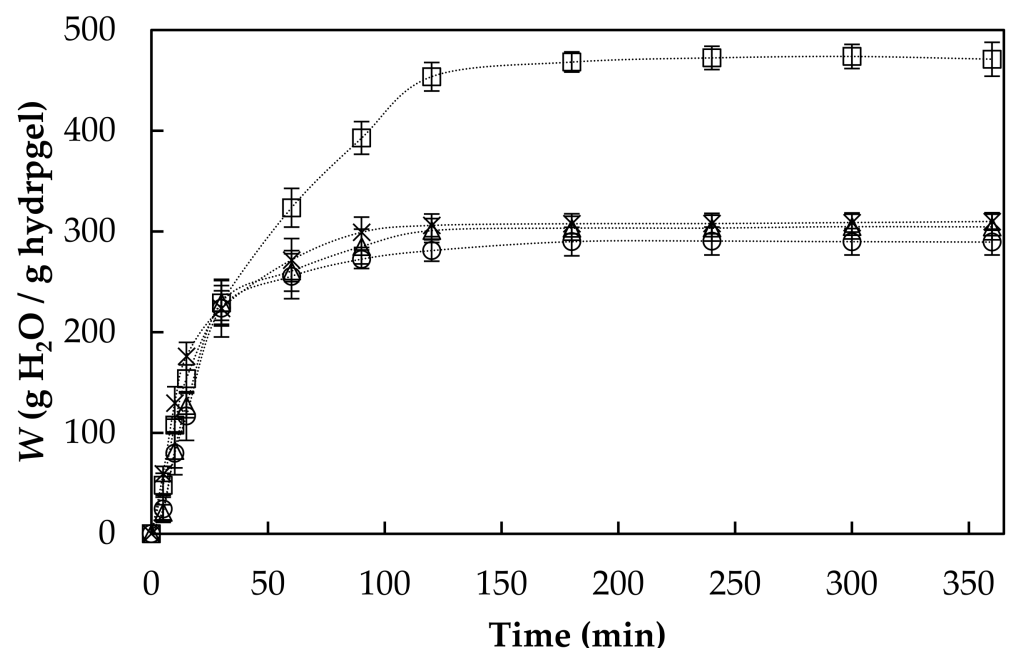


**Figure 1.** Swelling isotherms of non-reinforced acrylic hydrogels (AHR0, ×), and acrylic hydrogels reinforced with 3% *w/w* (AHR3, □), 5% *w/w* (AHR5, Δ), and 10% *w/w* (AHR10, ○) fique nanofiber.

As seen in Figure 1, there was a rapid increase in the degree of swelling at the beginning of all treatments, with similar swelling behavior during the first 30 min. For all samples, about 90% of the equilibrium value ( $W_{eq}$ ) was reached at about 90 min, followed by a slower process, until the equilibrium swelling ratio ( $W_{eq}$ ) was achieved at roughly

120 min of immersion. A trend similar to that found in this work has been reported in other studies [12,13,21].

On the other hand, Figure 2 shows the linear regression of the swelling curves obtained by Equation (2) for AHR0, AHR3, AHR5, and AHR10. The second-order kinetic relationship had a good fit since the correlation coefficients ( $R^2$ ) were 0.99 in all cases.

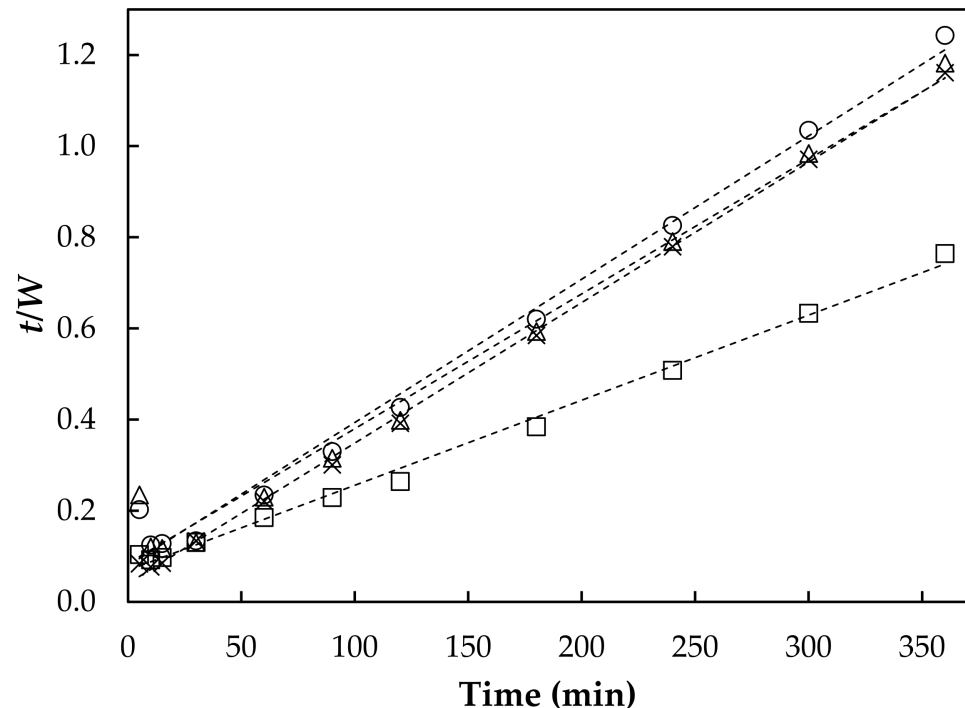


**Figure 2.** Swelling rate curves of AHR0 (×), AHR3 (□), AHR5 (Δ), and AHR10 (○).

The values associated with parameters of Equations (2)–(5) and calculated from the slope and the intersection of the lines in Figure 2 are presented in Table 1, where it can be seen that hydrogels reinforced with nanofibers (AHR3, AHR5, and AHR10) had lower values of  $K_s$  and  $K_{is}$ , which indicated that their swelling would occur more rapidly. This was due to the fact that AHR0 had a greater free volume between the polymeric networks [12,13,28].

**Table 1.** Parameters of the swelling kinetic.

Hydrogel	* $W_{eq}$	** $W_t$	*** $k_s \times 10^{-4}$	**** $k_{is}$
AHR0	310 ± 9 <sup>b</sup>	324	2.4	24.8
AHR3	474 ± 12 <sup>c</sup>	536	0.5	14.4
AHR5	305 ± 12 <sup>a,b</sup>	338	1.0	11.8
AHR10	291 ± 14 <sup>a</sup>	318	1.2	12.6

Different lowercase letters within the same column represent statistically significant differences at a 5% significance ( $p \leq 0.05$ ); \* Equilibrium swelling (g H<sub>2</sub>O g hydrogel<sup>-1</sup>); \*\* Equilibrium theoretical swelling (g H<sub>2</sub>O g hydrogel<sup>-1</sup>); \*\*\* Rate of swelling ((g H<sub>2</sub>O g hydrogel<sup>-1</sup>) min<sup>-1</sup>); \*\*\*\* Initial swelling constant ((g H<sub>2</sub>O g hydrogel<sup>-1</sup>) min<sup>-1</sup>).

It can be seen in Figure 1 that after 30 min, there was a much greater increase in AHR3 swelling. This could be corroborated in Table 1, since the equilibrium swelling ratio order was AHR3 > AHR0 > AHR5 > AHR10. Evidently, AHR3 had the best swelling capacity, despite being the least reinforced acrylic hydrogel.

The incorporation of fique nanofibers in hydrogels increases hydrophilic groups, thereby improving the diffusion of liquids into the matrix, and leading to the formation of pores in the polymer structure. Indeed, this addition reduces the hydrogel crossing points and enlarges the network voids, promoting the permeation of water into the polymeric

network [12]. In this work, increasing the concentration of nanofibers up to AHR3 led to increased interactions between the nanofibers and the polymer matrix, favoring the stability of the network, as mentioned above. However, beyond AHR3, and thus at a higher concentration of nanofibers, a higher viscosity of the reactive system could have been obtained, which could have brought about a reduction in the mobility of the polymer chains, thus disfavoring the crosslinking process. This phenomenon has already been reported by other studies [22,23,29].

### 3.2. Mechanical Properties

Table 2 shows the maximum compression resistance ( $R_C$ ) and strain percent of AHR0, AHR3, AHR5, and AHR10. Finding the appropriate nanofiber concentration to improve the mechanical properties of acrylic hydrogels is very important. An accurate nanofiber concentration ensures the dispersion of nanofibers within the polymeric network, thus obtaining hydrogels with higher strength. Authors such as Zhou et al. [23] indicated that uniformly dispersed nanofibers in the hydrogel support higher loadings due to the strong interfacial adhesion between the polymer chain chemically bonded to the -OH groups of the nanofibers (see Figure S1). In this work, it was found that the addition of fique nanofibers increased both  $R_C$  and strain percent properties of hydrogels. However, concentrations of fique nanofibers higher than 5% (>AHR5) decreased the mechanical properties of the reinforced hydrogels. This behavior, which is in agreement with what was discussed in the previous section above, could be due to the fact that an excess of nanofibers could lead to an inhomogeneous dispersion of the nanofibers in the reactant solution due to the increase in their viscosity, with consequent phase separation [29]. A similar phenomenon took place in the work reported by Zhou et al. [23].

**Table 2.** Maximum compression resistance ( $R_C$ ) and strain percent of hydrogels.

Hydrogel	$R_C$ (kPa)	Strain (%)
AHR0	$6 \pm 2^a$	$5 \pm 1$
AHR3	$8 \pm 3^{a,b}$	$6 \pm 1$
AHR5	$16 \pm 4^c$	$25 \pm 2$
AHR10	$10 \pm 1^b$	$17 \pm 2$

Different lowercase letters within the same column represent statistically significant differences at a 5% significance ( $p \leq 0.05$ ).

### 3.3. Morphologies of Hydrogels

Figure 3 shows SEM micrographs of non-lyophilized (Figure 3, left) and lyophilized (Figure 3, right) hydrogels synthesized in this work via the solution polymerization method. In general, the surface of the nanofiber-reinforced hydrogels (AHR3, AHR5, and AHR10) showed characteristic roughness (see Figure 3b–d), while the unreinforced hydrogel (AHR0) showed a smooth surface (see Figure 3a). In addition, Figure 3 (right) shows that, compared to AHR0, the morphology of the nanofiber-reinforced hydrogels (AHR3, AHR5, and AHR10) became much more irregular after freeze drying (see Figure 3b–d, right); even the presence of some pores formed during water swelling was noted. These pores were much more evident in AHR3 (Figure 3b, right), which is consistent with the greater capacity of this formulation to absorb water, placing it once again as the best candidate.

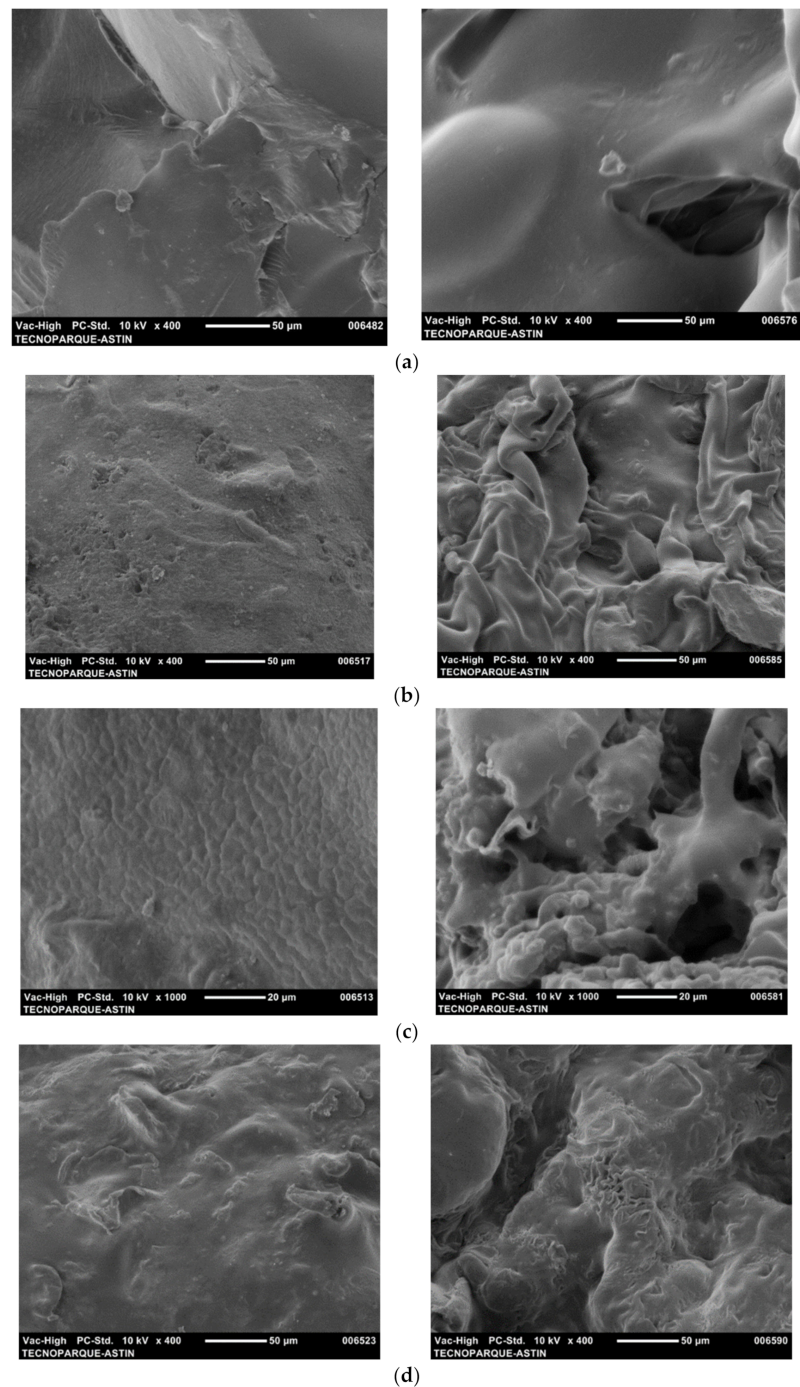


**Figure 3.** Scanning electron micrographs (SEM) of non-lyophilized (left) and lyophilized (right) hydrogels: (a) AHR0, (b) AHR3, (c) AHR5, and (d) AHR10.

#### 4. Conclusions

Based on a circular economy model, this work proposes a feasible option to revalue up to 7500 tons of waste per year from the Colombian figue agroindustry [25,26].

Today, Colombia uses roughly 40,000 million cubic meters of water in the agricultural sector. This demand is unsustainable; therefore, it is worth considering technologies focused on reducing the use of water for irrigation, increasing its availability in the soil for a longer period, and allowing for the efficient use of fertilizers.

The reinforced hydrogel with figue nanofibers at 3% *w/w* (AHR3) had the best swelling capacity in addition using the least amount of figue, which represents better economic benefits for industrial-scale production. The proposed superabsorbent hydrogel (AHR3)

could be used as an alternative to improve the water retention capacity of soils, reducing irrigation frequency by up to 90%. In addition, it would help to improve soil compaction and reduce water loss by infiltration and fertilizer loss. With the above, seed germination would be improved, thus increasing plant growth and delaying wilting in drought conditions, which are very common in some areas of Colombia such as the Department of Cesar, which is an issue that will worsen over the years due to the climate emergency.

**Supplementary Materials:** The following supporting information can be downloaded at: <https://www.mdpi.com/article/10.3390/agriculture12010117/s1>, Figure S1: Infrared spectrum (FIR) of non-reinforced acrylic hydrogels (AHR0), and acrylic hydrogels reinforced with 3% *w/w* (AHR3), 5% *w/w* (AHR5), and 10% *w/w* (AHR10) fique nanofiber.

**Author Contributions:** Conceptualization, M.A.G.-C., L.S.-C. and D.F.T.; data curation, M.A.G.-C., L.S.-C. and D.F.T.; formal analysis, M.A.G.-C., L.S.-C. and D.F.T.; funding acquisition, M.A.G.-C., L.S.-C. and D.F.T.; investigation, M.A.G.-C.; methodology, M.A.G.-C., L.S.-C. and D.F.T.; project administration, L.S.-C. and D.F.T.; resources, M.A.G.-C., L.S.-C. and D.F.T.; software, M.A.G.-C., L.S.-C. and D.F.T.; supervision, L.S.-C. and D.F.T.; validation, L.S.-C. and D.F.T.; visualization, D.F.T.; writing—original draft, M.A.G.-C., L.S.-C. and D.F.T.; writing—review and editing, D.F.T. All authors have read and agreed to the published version of the manuscript.

**Funding:** This research was funded by ASTIN-SENA (project reference 11796).

**Institutional Review Board Statement:** Not applicable.

**Informed Consent Statement:** Not applicable.

**Data Availability Statement:** The data that support the findings of this study are available on request from all authors.

**Acknowledgments:** The authors would like to thank to biotechnology laboratories of Tecnoparque Nodo Cali.

**Conflicts of Interest:** The authors declare no conflict of interest. The funders had no role in the design of the study; in the collection, analyses, or interpretation of data; in the writing of the manuscript, or in the decision to publish the results.

## References

1. United Nations. *World Population Prospects the 2017 Revision: Key Findings and Advance Tables*; United Nations: New York, NY, USA, 2017; p. 53.
2. United Nations. Sustainable Development Goals. Available online: <https://www.un.org/sustainabledevelopment/hunger/>. (accessed on 10 January 2021).
3. van Dijk, M.; Morley, T.; Rau, M.L.; Saghai, Y. A meta-analysis of projected global food demand and population at risk of hunger for the period 2010–2050. *Nat. Food* **2021**, *2*, 494–501. [[CrossRef](#)]
4. Hyánková, E.; Křiška Dunajský, M.; Zedník, O.; Chaloupka, O.; Pumprlová Němcová, M. Irrigation with treated wastewater as an alternative nutrient source (for crop): Numerical simulation. *Agriculture* **2021**, *11*, 946. [[CrossRef](#)]
5. Wilson, M.G.; Maggi, A.E.; Castiglioni, M.G.; Gabioud, E.A.; Sasal, M.C. Conservation of ecosystem services in argiudolls of Argentina. *Agriculture* **2020**, *10*, 649. [[CrossRef](#)]
6. Kostrzewska, M.K.; Jastrzębska, M.; Treder, K.; Wanic, M. Phosphorus in spring barley and Italian rye-grass biomass as an effect of inter-species interactions under water deficit. *Agriculture* **2020**, *10*, 329. [[CrossRef](#)]
7. Pérez-Blanco, C.D.; Hrast-Essenfelder, A.; Perry, C. Irrigation technology and water conservation: A review of the theory and evidence. *Rev. Environ. Econ. Policy* **2020**, *14*, 216–239. [[CrossRef](#)]
8. Mehana, M.; Abdelrahman, M.; Emadeldin, Y.; Rohila, J.S.; Karthikeyan, R. Impact of genetic improvements of rice on its water use and effects of climate variability in Egypt. *Agriculture* **2021**, *11*, 865. [[CrossRef](#)]
9. Yang, Q.; Hu, C.; Li, J.; Yi, X.; He, Y.; Zhang, J.; Sun, Z. A separation and desalination process for farmland saline-alkaline water. *Agriculture* **2021**, *11*, 1001. [[CrossRef](#)]
10. Haque, A.N.A.; Uddin, M.K.; Sulaiman, M.F.; Amin, A.M.; Hossain, M.; Solaiman, Z.M.; Mosharraf, M. Biochar with alternate wetting and drying irrigation: A potential technique for paddy soil management. *Agriculture* **2021**, *11*, 367. [[CrossRef](#)]
11. Feng, W.; Gao, J.; Cen, R.; Yang, F.; He, Z.; Wu, J.; Miao, Q.; Liao, H. Effects of polyacrylamide-based super absorbent polymer and corn straw biochar on the arid and semi-arid salinized soil. *Agriculture* **2020**, *10*, 519. [[CrossRef](#)]
12. Spagnol, C.; Rodrigues, F.H.A.; Neto, A.G.V.C.; Pereira, A.G.B.; Fajardo, A.R.; Radovanovic, E.; Rubira, A.F.; Muniz, E.C. Nanocomposites based on poly(acrylamide-co-acrylate) and cellulose nanowhiskers. *Eur. Polym. J.* **2012**, *48*, 454–463. [[CrossRef](#)]

13. Spagnol, C.; Rodrigues, F.; Pereira, A.; Fajardo, A.; Rubira, A.; Muniz, E. Superabsorbent hydrogel composite made of cellulose nanofibrils and chitosan-graft-poly(acrylic acid). *Carbohydr. Polym.* **2012**, *87*, 2038–2045. [[CrossRef](#)]
14. Li, J.; Jia, X.; Yin, L. Hydrogel: Diversity of structures and applications in food science. *Food Rev. Int.* **2021**, *37*, 313–372. [[CrossRef](#)]
15. Song, B.; Liang, H.; Sun, R.; Peng, P.; Jiang, Y.; She, D. Hydrogel synthesis based on lignin/sodium alginate and application in agriculture. *Int. J. Biol. Macromol.* **2020**, *144*, 219–230. [[CrossRef](#)]
16. Qu, B.; Luo, Y. Chitosan-based hydrogel beads: Preparations, modifications and applications in food and agriculture sectors — A review. *Int. J. Biol. Macromol.* **2020**, *152*, 437–448. [[CrossRef](#)]
17. Mohite, S.; Prasad, E. *Hydrogel Market Outlook - 2027*; Allied Market Research: Pune, India, 2020; p. 363.
18. Serna Cock, L.; Guancha-Chalapud, M.A. Natural fibers for hydrogels production and their applications in agriculture. *Acta Agron.* **2017**, *66*, 495–505. [[CrossRef](#)]
19. Das, D.; Prakash, P.; Rout, P.K.; Bhaladhare, S. Synthesis and characterization of superabsorbent cellulose-based hydrogel for agriculture application. *Starch - Stärke* **2021**, *73*, 1900284. [[CrossRef](#)]
20. Huang, Y.; Li, X.; Lu, Z.; Zhang, H.; Huang, J.; Yan, K.; Wang, D. Nanofiber-reinforced bulk hydrogel: Preparation and structural, mechanical, and biological properties. *J. Mater. Chem. B* **2020**, *8*, 9794–9803. [[CrossRef](#)]
21. Karadag, E.; Baris, O.; Saraydin, D. Water uptake in chemically crosslinked poly(acrylamide-co-crotonic acid) hydrogels. *Mater. Des.* **2005**, *26*, 265–270. [[CrossRef](#)]
22. Zhou, C.; Wu, Q. A novel polyacrylamide nanocomposite hydrogel reinforced with natural chitosan nanofibers. *Colloids Surfaces B Biointerfaces* **2011**, *84*, 155–162. [[CrossRef](#)]
23. Zhou, C.; Wu, Q.; Yue, Y.; Zhang, Q. Application of rod-shaped cellulose nanocrystals in polyacrylamide hydrogels. *J. Colloid Interface Sci.* **2011**, *353*, 116–123. [[CrossRef](#)] [[PubMed](#)]
24. Guancha-Chalapud, M.A.; Gálvez, J.; Serna-Cock, L.; Aguilar, C.N. Valorization of Colombian fique (*Furcraea bedinghausii*) for production of cellulose nanofibers and its application in hydrogels. *Sci. Rep.* **2020**, *10*, 11637. [[CrossRef](#)]
25. Ovalle-Serrano, S.A.; Gómez, F.N.; Blanco-Tirado, C.; Combariza, M.Y. Isolation and characterization of cellulose nanofibrils from Colombian Fique decortication by-products. *Carbohydr. Polym.* **2018**, *189*, 169–177. [[CrossRef](#)]
26. Ovalle-Serrano, S.A.; Blanco-Tirado, C.; Combariza, M.Y. Exploring the composition of raw and delignified Colombian fique fibers, tow and pulp. *Cellulose* **2018**, *25*, 151–165. [[CrossRef](#)]
27. Zhong, K.; Zheng, X.-L.; Mao, X.-Y.; Lin, Z.-T.; Jiang, G.-B. Sugarcane bagasse derivative-based superabsorbent containing phosphate rock with water–fertilizer integration. *Carbohydr. Polym.* **2012**, *90*, 820–826. [[CrossRef](#)] [[PubMed](#)]
28. Spagnol, C.; Rodrigues, F.; Pereira, A.; Fajardo, A.; Rubira, A.; Muniz, E. Superabsorbent hydrogel nanocomposites based on starch- g -poly ( sodium acrylate) matrix filled with cellulose nanowhiskers. *Cellulose* **2012**, *19*, 1225–1237. [[CrossRef](#)]
29. Yang, J.; Han, C.R.; Duan, J.F.; Xu, F.; Sun, R.C. Mechanical and viscoelastic properties of cellulose nanocrystals reinforced poly(ethylene glycol) nanocomposite hydrogels. *ACS Appl. Mater. Interfaces* **2013**, *5*, 3199–3207. [[CrossRef](#)] [[PubMed](#)]